Electronic Supplementary Material (ESI) for Nanoscale Horizons.

Supporting Information

Lead-Free, Stable, High-efficiency (52%) Blue luminescent $FA_3Bi_2Br_9$ Perovskite Quantum Dots

Yalong Shen,[a] Jun Yin,[b] Bo Cai,[a] Ziming Wang,[a] Yuhang Dong,[a] Xiaobao Xu,[a] Haibo Zeng[a,*]

[a] MIIT Key Laboratory of Advanced Display Materials and Devices, Institute of Optoelectronics & Nanomaterials, College of Materials Science and Engineering, Nanjing University of Science and Technology. Nanjing 210094, China
[b] Division of Physical Sciences and Engineering, King Abdullah University of Science and Technology, Thuwal 23955-6900, Kingdom of Saudi Arabia

*Author to whom correspondence should be addressed: zeng.haibo@njust.edu.cn.

Experimental section:

Chemicals; $BiBr_3$ (99%, Alfa Aesar), formamidine acetate (99%, Aladdin), oleylamine (OAm, 90%, Aladdin), oleic acid (OA, 90%, Aladdin), N,N-Dimethylformamide (DMF, 99%, Aladdin), ethyl acetate (Aladdin), dimethyl sulfoxide (DMSO, 99%, Aladdin), hydroiodic acid (HI, 48 wt% in water, Meryer) , hydrobromic acid (HBr, 48 wt% in water, Meryer), hydrochloric acid (HCl, 37 wt% in water, sinopharm Chemical Reagent Co., Ltd, China), ethanol anhydrous (99.8%, Aladdin), toluene (anhydrous, 99.5%, sinopharm Chemical Reagent Co., Ltd, China), Polystyrene (PS, M_w ~280000, Meryer). All the materials were used as purchase without any further purifications.

Synthesis of FAX (X= Cl, Br or I); Formamidine acetate was dissolved in 2 molar equivalents of HBr in a 250 mL round-bottomed flask at 0 °C for 30min stirring. The reaction solution was stirred until the formamidine acetate is deliquescent. The solution was removed at 100 °C by means of rotary evaporator. The FABr product was washed with diethyl ether by stirring the solution for 30 min, followed by drying in a vacuum oven for 24h (60 °C) and then stored in a glove box. The FACl and FAI were obtained by reaction of the formamidine acetate with HCl and HI, respectively.

Preparation of $FA_3Bi_2X_9$ QDs: In a typical synthesis of $FA_3Bi_2Br_9$ QDs, we used a mixture solution of N,N-Dimethylformamide (DMF) and dimethyl sulfoxide (DMSO) as the "good" solvent to dissolve FABr and ethyl acetate to dissolve $BiBr_3$. 0.4 mmol of FABr was dissolved into 2 mL of mixed solution containing 1.8 mL of DMF and 0.2 mL of DMSO, while 0.268 mmol of $BiBr_3$ was dissolved in 2 mL ethyl acetate, the above process were operated in the glove box. Then, 25 uL of oleylamine was added to stabilize the precursor. After that, 0.5 mL precursor solution was quickly injected into a mixture containing 5 mL of toluene and 0.65 mL of OA under vigorous stirring. The reaction mixture was centrifuged at 8000 rpm for 5 min to discard the precipitates containing large particles. Subsequently, a clear pale-yellow colloidal $FA_3Bi_2Br_9$ resultant supernatant was obtained, which yields the final product for further use and characterization. The solid powder of $FA_3Bi_2Br_9$ QDs was obtained by rotary evaportating the residual organic solvents at 85 °C. The $FA_3Bi_2Cl_9$ and $FA_3Bi_2I_9$ QDs were synthesized *via* the same method by varying the precursor solutions. Typically, mixed halide perovskites $FA_3Bi_2(Cl_{0.5}Br_{0.5})_9$ and $FA_3Bi_2(I_{0.5}Br_{0.5})_9$ were fabricated with the mixture of BiX_3 and FAX (X = Cl, Br and I).

Fabrication of the blue LED device: Condensed $FA_3Bi_2Br_9$ QDs solution was mixed with PS/toluene solution (0.15g/mL). The mixed solution was then dropped into the LED cap and cured in a vacuum oven for 60 min, which was painted on the surface of the UV light chip.

Material characterizations: The crystalline phase and structure of the samples was characterized by XRD (Bruker-AXS D8 Advance). UV/Vis absorption spectra of films were measured by using a Shimadzu 3600 UV/Vis spectrophotometer. Photoluminescence spectra were obtained via Varian Cary Eclipse instrument. The morphology and microstructures were obtained using TEM (FEI Tecnai G20) and HRTEM (FEI Tecnai G20). Time-resolved PL decay was measured by an Optronics streak camera system with optimized temporal resolution of ≈ 50 ps. The PLQY was determined using a Quantauru-QY Absolute photoluminescence quantum yield spectrometer (C11347-11, Hamamatsu Photonics, Japan). X-ray photoelectron spectroscopy (XPS) measurements were performed using an achromatic Al Kα source (1486.6 eV) and a double pass cylindrical mirror analyzer (PHI QUANTERA II)

Computational Details: Density functional theory (DFT) calculations were performed with a generalized gradient approximation (GGA)/Perdew-Burke-Ernzerhof (PBE) level using the projector-augmented wave (PAW) method, as implemented in the VASP code[1, 2]. The crystal structure of $FA_3Bi_2Br_9$ was built following the hexagonal-phase $MA_3Bi_2Br_9$ by replacing MA cations with FA cations[3], and then the crystal structure of $FA_3Bi_2Br_9$ was further optimized by fully relaxing both the lattice and atomic positions. The *k*-points grid of 6×6×6 over the Brillouin zone was used during the crystal structure optimization and electronic properties calculations. The electronic plane-wave cutoff energy was set to 500 eV. The crystal geometry of $FA_3Bi_2Br_9$ was optimized until all forces on all atoms were smaller than 0.01 eV/Å.

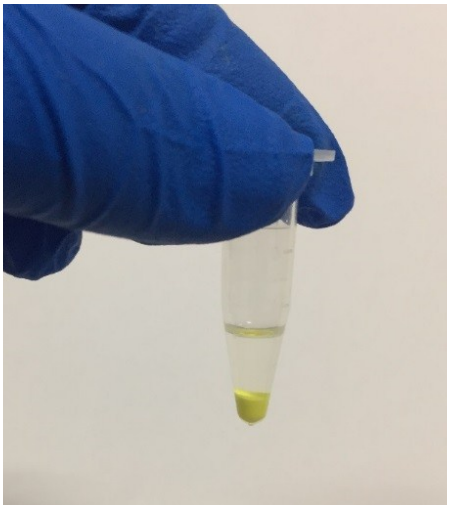

Figure S1. The image of the $FA_3Bi_2Br_9$ powder in toluene prepared from rotary evaporation.

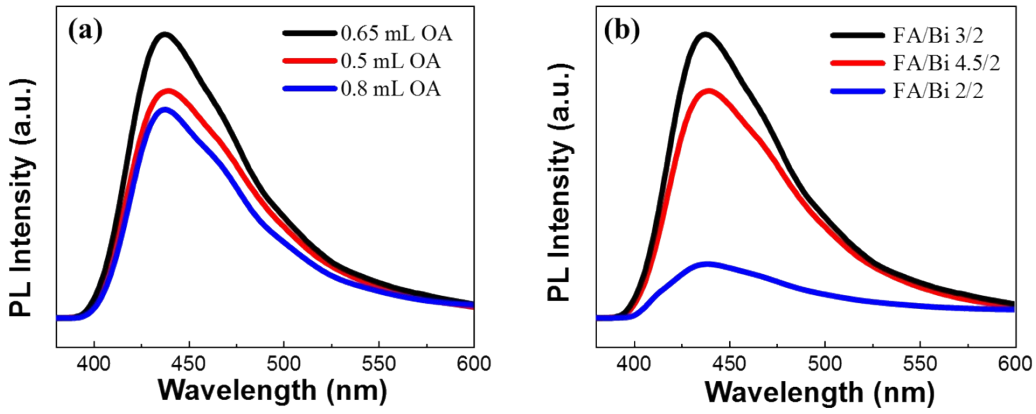

Figure S2. PL spectra of the prepared $FA_3Bi_2Br_9$ QDs with (a) different amounts of OA added and (b) the ratios of FA:Bi.

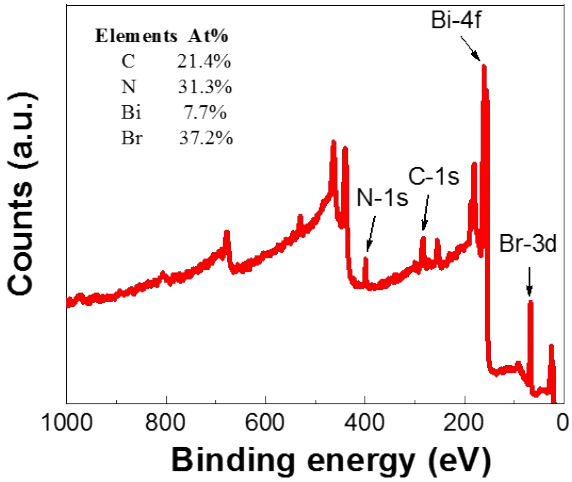

Figure S3. X-ray photoelectron spectrum (XPS) of $FA_3Bi_2Br_9$ QDs measured under ambient conditions.

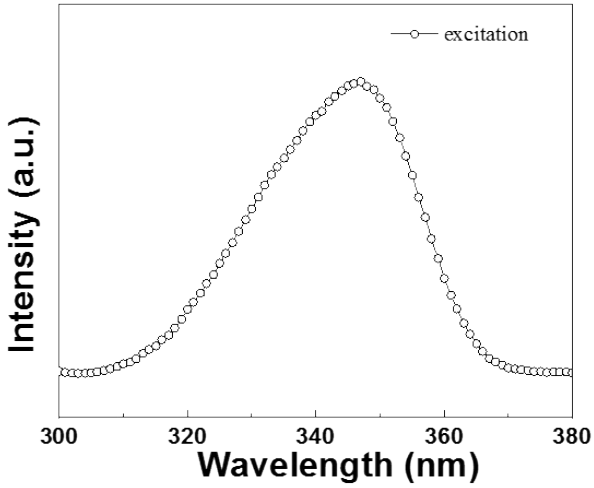

Figure S4. PL excitation spectra of $FA_3Bi_2Br_9$ QDs

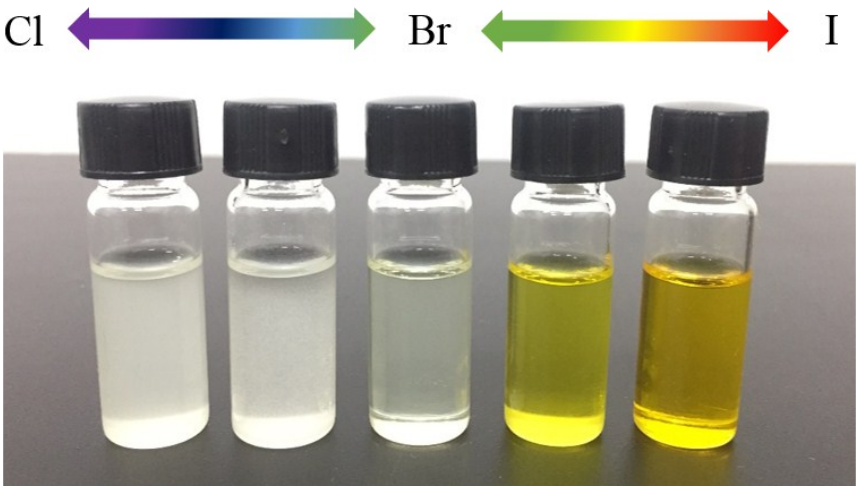

Figure S5. Photographs of the as-obtained colloidal $FA_3Bi_2X_9$ QDs (X= Cl, Br, and I).

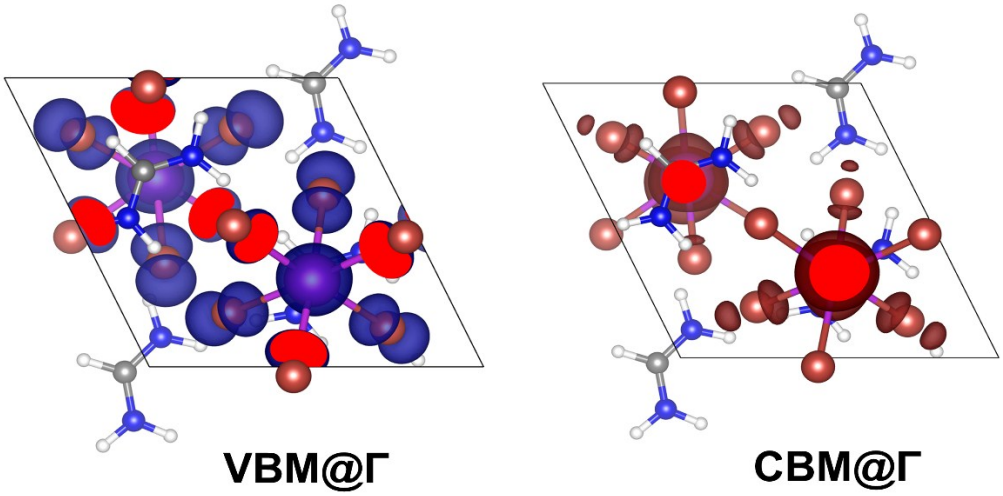

Figure S6. Charge density distributions for valence band maximum (VBM) and conduction band minimum (CBM) at symmetric Γ-point of $FA_3Bi_2Br_9$.

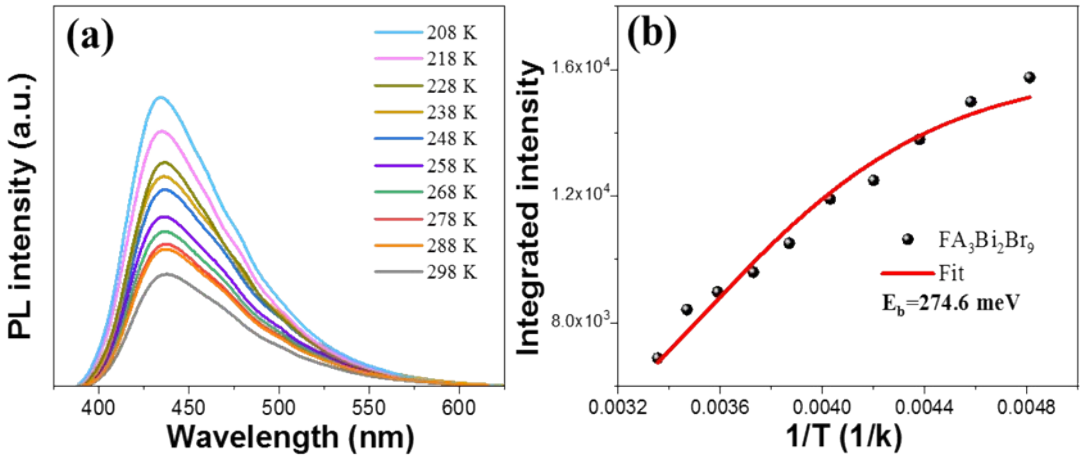

Figure S7. (a) Temperature-dependent PL spectra of $FA_3Bi_2Br_9$ QDs. (b) Integrated PL emission intensity as a function of temperature from 208 to 298 K.

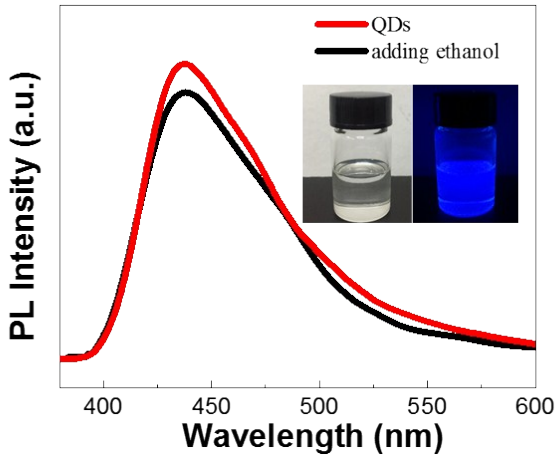

Figure S8. The stability of $FA_3Bi_2Br_9$ QDs after adding 1 mL ethanol anhydrous into 1 mL QDs solution. The insets: photographs of the $FA_3Bi_2Br_9$ QDs solutions after adding ethanol under visible and UV light.

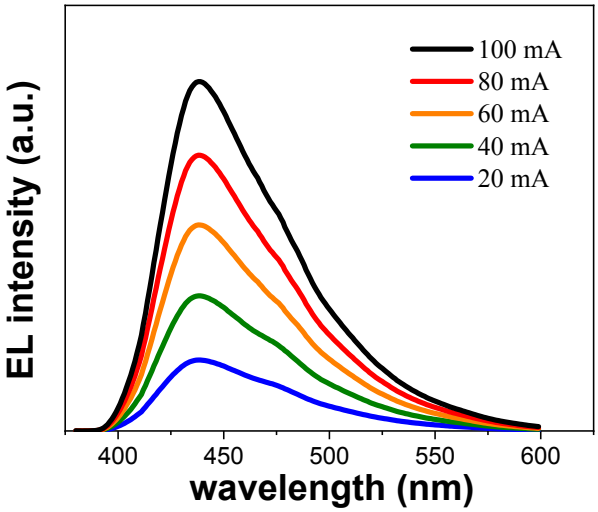

Figure S9. EL spectra of the blue LED under increased operating currents.

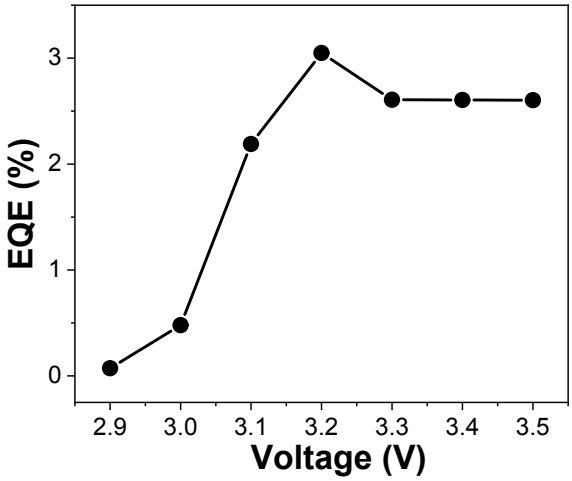

Figure S10: Plot of the LED EQE as a function of the driving voltage.

Table S1. Properties comparison of different blue luminescent lead-free perovskites QDs.

QDs	PL peak (nm)	FWHM (nm)	PLQY (%)	E_b (meV)	Ref
$FA_3Bi_2Br_9$	437	65	52	274.6	This work
$MA_3Bi_2Br_9$	423	62	12	-	3
Cl-$MA_3Bi_2Br_9$	422	41	54	259.1	4
$Cs_3Bi_2Br_9$	410	48	19.4	210.7	5
$Cs_3Bi_2Br_9$	468	40	4.5	-	6
$Cs_3Sb_2Br_9$	410	41	46	548	7

Table S2. Summary of PL peaks, FWHM, PLQY and bandgaps of colloidal $FA_3Bi_2X_9$ (X= Cl, Br and I) QDs.

QDs	PL peak (nm)	FWHM (nm)	PLQY (%)	Bandgap (eV)
$FA_3Bi_2Cl_9$	399	63	39	3.09
$FA_3Bi_2Br_9$	437	65	52	2.87
$FA_3Bi_2I_9$	526	67	0.2	2.46

Table S3. Comparison of different blue LEDs based on perovskites.

Type	Materials	PLQY (%)	PL peak (nm)	EL peak (nm)	EQE (%)	Ref
Backlit LED	$FA_3Bi_2Br_9$ QDs	52	437	437	3.05	This work
Backlit LED	Bi-Gd_2ZnTiO_6 Phosphor	-	419	419	-	8
Backlit LED	Cs_4PbBr_6/$CsPbCl_3$ NCs	90	463	463	-	9
EL LED	Mn-$CsPb(Cl/Br)_3$ NCs	28	468	466	2.12	10
EL LED	$CsPbBr_3$ NPs	96	463	463	0.124	11
EL LED	$CsPb(Cl/Br)_3$ NCs	＞50	469	469	0.5	12
EL LED	$PEA_2Cs_{n-1}Pb_n$ $(Cl_xBr_{1-x})_{3n+1}$	27	Broad	480	5.7	13

One thing to note here is the comparison of EQE. EQE is regarded as the most important parameter of electroluminescent (EL) perovskite-based LEDs, but rarely used to characterize backlit LEDs, because the commercial chip act as excitation light source in backlit LEDs could affect the device EQE, and thus the achieved EQE value cannot reflect the intrinsic properties of perovskites. So, the direct comparison of EQE between the backlit LEDs and EL LEDs needs to be viewed accordingly.

References

1. G. Kresse and D. Joubert, *Phys. Rev. B*, 1999, **59**, 1758-1775.
2. G. Kresse and J. Furthmüller, *Comput. Mater. Sci*, 1996, **6**, 15-50.
3. M. Leng, Z. Chen, Y. Yang, Z. Li, K. Zeng, K. Li, G.Niu, Y. He, Q.Zhou and J. Tang, *Angew. Chem., Int. Ed*, 2016, **55**, 15012-15016.
4. M. Leng, Y. Yang, Z. Chen, W. Gao, J. Zhang, G. Niu, D. Li, H. Song, J. Zhang, S. Jin and J. Tang, *Nano Lett.*, 2018, **18**, 6076-6083.
5. M. Leng, Y. Yang, K. Zeng, Z. Chen, Z. Tan, S. Li, J. Li, B. Xu, D. Li, M. P. Hautzinger, Y. Fu, T. Zhai, L. Xu, G. Niu, S. Jin and J. Tang, *Adv. Funct. Mater.,* 2018, **28**, 1704446
6. B. Yang, J. Chen, F. Hong, X. Mao, K. Zheng, S. Yang, Y. Li, T. Pullerits, W. Deng and K. Han, *Angew. Chem. Int. Ed.*, 2017, **56**, 12471-12475.
7. J. Zhang, Y. Yang, H. Deng, U. Farooq, X. Yang, J. Khan, J. Tang and H.Song, *ACS Nano*, 2017, **11**, 9294-9302.
8. C. Ji, Z. Huang, J. Wen, J. Zhang, X. Tian, H. He, L. Zhang, T. Huang, W. Xie and Y. Peng, *J. Alloys Compd.*, 2019, **788**, 1127-1136.
9. C. Sun, C. Gao, H. Liu, L. Wang, Y. Deng, P. Li, H. Li, Z. Zhang, C. Fan and W. Bi, *Chem. Mater.*, 2019, **31**, 5116−5123
10. S. Hou, M.K. Gangishetty, Q. Quan and D.N. Congreve, *Joule.*, 2018, **2**, 2421-2433.
11. Y. Wu, C. Wei, X. Li, Y. Li, S. Qiu, W. Shen, B. Cai, Z. Sun, D. Yang, Z. Deng and and H. Zeng, *ACS Energy Lett.*, 2018, **3**, 2030-2037.
12. M.K. Gangishetty, S. Hou, Q. Quan and D.N. Congreve, *Adv. Mater.*, 2018, **30**, 1706226.
13. Z. Li, Z. Chen, Y. Yang, Q. Xue, H. L. Yip, Y. Cao, *Nat. Commun.*, 2019, **10**, 1027.